First experimental results of the use of R1234yf and R1234ze(E) as drop-in substitutes for R134a in a water-to-water heat pump

L Molinaroli[1], A Lucchini[1], LPM Colombo[1] and F Bocchinfuso[1]

[1] Dipartimento di Energia, Politecnico di Milano, via Raffaele Lambruschini 4/A, 20156, Milano (MI), Italy
Corresponding author e-mail: luca.molinaroli@polimi.it

Abstract. In the present paper, the first results of an experimental analysis carried out to assess the performance of a water-to-water heat pump in which R1234yf and R1234ze(E) are used as drop-in substitutes of R134a are shown. The heat pump is first tested with R134a to establish a baseline performance and, then, is tested under the same working conditions, i.e. under the same water temperatures at evaporator and condenser outlets, with the above-mentioned HFO refrigerants. The results show that the heating capacity and COP of R1234yf system are up to 9.8% and 6.1% respectively lower than those obtained with R134a. On the other side, the use of R1234ze(E) leads to a capacity reduction and a COP reduction respectively up to 23.1% and 2.5%. A second set of tests is then carried out varying the rotational frequency of the compressor shaft in order to set the heat pump heating capacity to the same value found with R134a. The experimental results demonstrate that increases up to 17% and 50% are respectively needed for R1234yf and R1234ze(E), but subsequent reductions of heat pump COP up to 7.38% and 18.11% arise.

1. Introduction

The recent EU 517/2014 regulation [1] and the Kigali amendment [2] have introduced constraints that force the air conditioning and refrigeration industry to find new refrigerants able to cope with more and more severe limits on Global Warning Potential (GWP). As a consequence, in the last years, new refrigerants have been continuously introduced and the need of testing them in vapour compression systems to analyse their performance arises. Among them, the HydroFluoroOlefins (HFO) R1234yf and R1234ze(E) have gained attention as substitutes of R134a.

Jaral [3] carried out a theoretical and an experimental analysis of the use of R1234yf in a water-to-water system. The theoretical analysis showed that R1234yf has lower pressure ratio, refrigerant temperature at compressor discharge and COP, while a reduction of cooling capacity and COP in the range 3.4% - 13.7% and 0.35% - 11.88% were experimentally measured.

Navarro-Esbrí et al. [4] carried out an extensive experimental analysis of the use of R1234yf in water-to-water vapour compression system in a drop-in application. They analysed the influence of evaporating temperature, condensing temperature, internal heat exchanger use, superheating degree and compressor drive frequency. They found that the use of R1234yf leads to an overall reduction of the cooling capacity, in the range 4.36% - 13.46%, and of the COP, in the range 5.60% - 27.89%, with larger differences at low evaporating or condensing temperatures. R1234yf benefited more than R134a from the use of internal heat exchanger while the influence of different superheating set-points or different compressor drive frequencies was negligible.

Mota-Babiloni et al. [5] experimentally assessed the performance of a water-to-water vapour compression system in a drop-in application of R134a, R1234yf and R1234ze(E). Three evaporating temperatures in the range 260 K – 280 K, three condensing temperatures in the range 310 K – 330 K were considered for a total of 9 experimental points per fluid. Additional 9 points were tested adding an internal heat exchanger to the system. Overall, it was observed that the use of R1234yf resulted in a cooling capacity reduction up to 13.71% and a COP reduction up to 10.50%, whereas the use of R1234ze(E) led to a cooling capacity reduction up to 33.68% and a COP reduction up to 8.40%.
Janković et al. [6] compared R134a, R1234yf and R1234ze(E) in a vapour compression system by means of a validated simulation tool. They found that, under the same evaporating and condensing temperatures, the cooling capacity of both HFOs is lower than that of R134a; with reduction equal to about 6% for R1234yf and 27% for R1234ze(E). On the other side, the COP of the system was about 1% lower for R1234ze(E) and from 2% to 5% lower for R1234yf. Vice-versa, under the same cooling medium conditions, i.e. same inlet and outlet condenser temperatures, R1234yf was found to perform worse than R134a both with respect to cooling capacity (5% - 9% reduction) and COP (7% - 10% reduction) whereas R1234ze(E) showed lower cooling capacity (about 25% reduction) but higher COP (4% - 7% increase) with respect to R134a.
Sánchez et al. [7] experimentally compared six different refrigerants in a direct drop-in application in a water-to-water system and, among them, R134a, R1234yf and R1234ze(E) were considered. They considered two evaporating temperatures, namely -10 °C and 0 °C, and three condensing temperatures, namely 25 °C, 35 °C and 45 °C, finding that the cooling capacity and the COP of the system using R1234yf were respectively reduced in the range 4.5% - 8.6% and 8.3% - 11.0% with respect to the R134a baseline. With the R1234ze(E), the cooling capacity and COP reduction were instead between 22.9% - 26.6% and 2.8% - 13.0% respectively.
Nawaz et al. [8] carried out an extensive numerical study with a validate simulation model of the use of R1234yf and R1234ze(E) as substitutes of R134a in heat pump water heaters. They concluded that the two HFOs lead to performances (first hour rating, unified energy factor and COP) slightly lower than those obtained with R134a. The charge of the system was found similar whereas the refrigerant temperature at compressor discharge was higher for R134a. Finally, R1234ze(E) required a larger compressor to overcome its lower volumetric heating capacity.
Finally, Devecioğlu and Oruç [9] experimentally analysed the influence of an internal heat exchanger in an air-to-air vapour compression system in which R1234yf and R1234ze(E) were used as drop-in substitutes of R134a. They found that the cooling capacity of the system using R134a was better than that of the system using R1234yf which, in turn, was better than that obtained with R1234ze(E). The capacity increased using the plate heat exchanger. Regarding the COP, R134a was the best refrigerants but R1234ze(E) performed better than R1234yf. Again, the use of the internal heat exchanger led to increased performance of the vapour compression system.
All the previous papers provide valuable information about the use of R1234yf and R1234ze(E) as R134a alternatives in vapour compression systems. The present study is aimed at contributing to this general discussion, presenting experimental results obtained using the "vapour compression system" point of view instead of the "refrigerant" point of view. Indeed, rather than keeping the evaporating and the condensing temperatures constant, as done in most of the experimental works reviewed above, in the present study the inlet and the outlet temperatures of the secondary fluids that flow through the evaporator and the condenser are fixed, so as to let the system to find its own operating point, that depends on the refrigerant used, the heat transfer area and the temperature levels of the cold heat source and hot heat sink.

2. Experimental set-up
Figure 1 depicts the layout of the experimental set-up used to assess the performance of R134a, R1234yf and R1234ze(E) in a drop-in application.

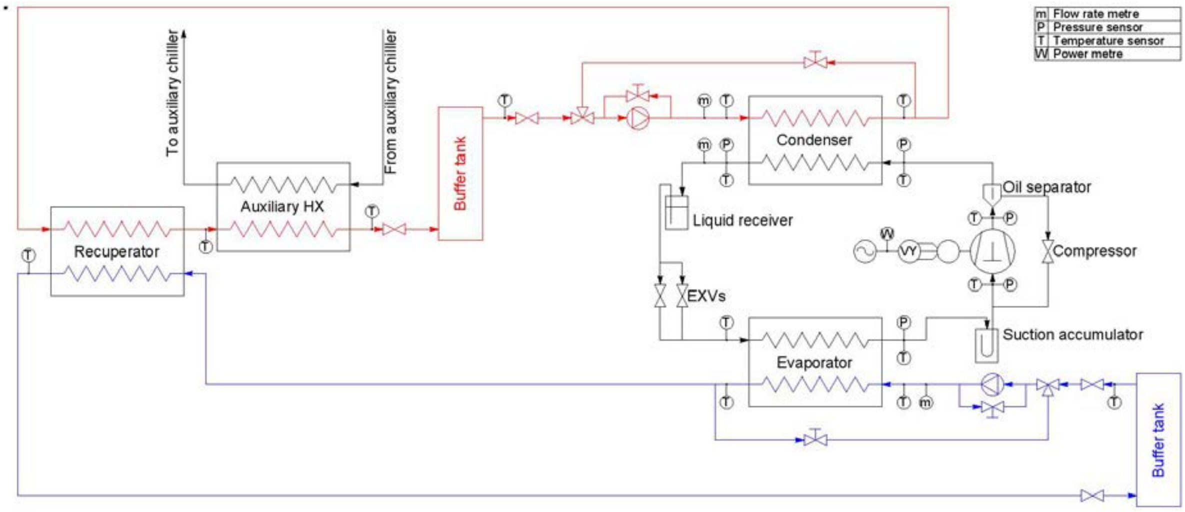

Figure 1. Layout of the experimental set-up.

The test rig mimics a water-to-water system and basically consists of three different loops: the refrigerant loop, the cold water + ethylene glycol loop and the hot water loop.
The main components of the refrigerant loop are a variable speed, semi-hermetic reciprocating compressor, two stainless steel plate heat exchangers (i.e. the condenser and the evaporator) and two electronic expansion valves (in parallel). Additional components for safe and smooth operation such as the suction accumulator, the oil separator and the liquid receiver are installed too. The refrigerant loop was controlled acting on the compressor shaft rotational frequency which, in turn, influences the circulating refrigerant mass flow rate, and on the set-point of the superheating at evaporator outlet.
The water + ethylene glycol loop consists of a variable speed pump, a buffer tank and a three-way valve. The cold water loop was controlled acting on pump rotational speed, to set the water + ethylene glycol flow rate to the desired value, and on the three-way valve, to set the mixture temperature at evaporator outlet to the required set-point. The buffer tank allowed to reduce the water + ethylene glycol temperature fluctuations and to reach stable testing conditions. The ethylene glycol concentration is 25.4% by volume that leads to freezing temperature equal to -12.6 °C.
Finally, the hot water loop is built considering the same components found in the water + ethylene glycol loop and adding an auxiliary chiller. Similarly to the cold loop, the hot water loop was used to set the water flow rate and the water temperature at condenser outlet to the desired values. Again, the buffer tank allowed to reduce the hot water temperature fluctuations and to reach stable testing conditions.
The main characteristics of the test rig components are provided in Table 1.

Table 1. Main characteristics of the experimental set-up components.

Component	Parameter	Range
Compressor	Swept volume @ 50 Hz	13.15 $m^3 \cdot h^{-1}$
	Shaft frequency	30 Hz – 87 Hz
Condenser	Height x Width x Depth	289 mm x 119 mm x 93.6 mm
	N° of plates	40
Evaporator	Height x Width x Depth	376 mm x 119 mm x 71.2 mm
	N° of plates	30
Expansion valves	Capacity range	1200 W - 12000 W
	Capacity range	1690 W - 16900 W
Liquid receiver	Volume	$2.8 \cdot 10^{-3}$ m^3
Suction accumulator	Volume	$2.33 \cdot 10^{-3}$ m^3
Oil separator	Volume	$2.8 \cdot 10^{-3}$ m^3

The test rig was equipped with instrumentations for the measurements of the main operating parameters such as pressures, temperatures, flow rates and power. Figure 1 shows the position of each measurement device whereas Table 2 depicts the main characteristics.

Table 2. Main characteristics of the measurement devices.

Parameter	Instrument	Range	Accuracy
Refrigerant mass flow rate	Coriolis mass flow metre	0 kg·h^{-1} – 300 kg·h^{-1}	± 0.15% r.v
Refrigerant pressure (low side)	Pressure transducer	0 kPa - 700 kPa	± 0.3% f.s
Refrigerant pressure (high side)	Pressure transducer	0 kPa - 4000 kPa	± 0.3% f.s
Refrigerant temperature	RTD Pt 100	243.15 K - 343.15 K	± 0.1 K
Compressor power	Power transducer	0 W - 4000 W	± 0.2% f.s
Water mass flow rate	Vortex flow metre	0.21 m^3·h^{-1} - 3 m^3·h^{-1}	± 2% r.v
Water temperature	RTD Pt 100	243.15 K - 343.15 K	± 0.1 K

2.1. Experimental procedure
The experimental used to run each test is the following:

1. The pumps of the cold water + ethylene glycol and of the hot water loops are switched on. The pump speeds are set to the values needed to guarantee the water mass flow rates required by the test.
2. The compressor is switched on and the shaft rotational frequency is set to the value required by the test.
3. The temperature of the secondary fluids at the outlet of evaporator and condenser that are required by the test are set acting on the 3-way valves. For each hydronic circuit, a PID controller keeps the outlet temperature to the set-point value during the test.
4. Once the set-point temperatures at heat exchanger outlets are reached, the data acquisition begins with a sample rate equal to 1 s. The simple moving average of the last 900 samples is calculated for each measured pressure and temperature.
5. If the deviation of each measured pressure and temperature lies respectively within ± 10 kPa and ± 0.2 K, the steady-state condition is considered to be achieved and further 900 samples are recorded for data analysis.
6. Finally, at the end of the test, the evaporator and condenser heat transfer rates are calculated considering both the refrigerant side and the secondary fluid side. If the two values agree within 4%, the test is considered completed otherwise it is repeated.

2.2. Data reduction and uncertainty calculation
The experimental set-up is operated as a heat pump, therefore the condenser capacity is the useful effect and the COP is the performance index.
The condenser capacity, is calculated as the average value between the refrigerant-side value and the water-side value as per the following equation:

$$\dot{Q}_{COND} = \frac{1}{2}\left[\dot{m}_R\left(h_{R,IN,COND} - h_{R,OUT,COND}\right) + \dot{m}_W c_{P,W}\left(T_{W,OUT,COND} - T_{W,IN,COND}\right)\right] \quad (1)$$

Refprop [10] software is used to calculate the refrigerant enthalpies, as function of refrigerant pressure and temperature, and the water isobaric heating capacity, as function of water average temperature.
The coefficient of performance is calculated neglecting the power consumption of the two pumps and the power consumption of the EXV controller as follows:

$$COP = \dot{Q}_{COND}/\dot{W}_{COMP} \quad (2)$$

where the compressor power accounts also for inverter losses.

The uncertainty of the above-mentioned quantities is estimated according to Moffat [11]. More in detail, the experimental uncertainty of each directly measured variable is calculated as follows:

$$u_x = \pm\left[u_{x,INST}^2 + (t_{95}\sigma_{\bar{x}})^2\right]^{1/2} \qquad (3)$$

Similarly, the uncertainty of the generic calculated quantity is estimated using the combined standard uncertainty under the uncorrelated input quantities assumption:

$$u_y = \pm\left[\sum_{i=1}^{N}\left(\frac{\partial y}{\partial x_i}u_{x,INST}\right)^2 + t_{95}^2\left(\frac{\partial y}{\partial x_i}\sigma_{\bar{x}}\right)^2\right]^{1/2} \qquad (4)$$

3. Experimental results

In the present study, three different refrigerants are tested, namely R134a and its low GWP alternatives, the HFOs R1234yf and R1234ze(E). The main characteristics of these refrigerants are reported in Table 3.

Table 3. Main properties of the three tested refrigerants.

Parameter	R134a	R1234yf	R1234ze(E)
Chemical formula	CH_2FCF_3	CF_3-CF=CH_2	$C_3H_2F_4$
Critical pressure	4059.3 kPa	3382.2 kPa	3634.9 kPa
Critical temperature	101.06 °C	94.7 °C	109.36 °C
Molar mass	102.03 g·mol^{-1}	114.04 g·mol^{-1}	114.04 g·mol^{-1}
Normal Boiling Point	-26.074 °C	-29.45 °C	-18.973 °C
ODP	0	0	0
GWP_{100} [12]	1300	< 1	< 1
ASHRAE Classification	A1	A2L	A2L

For each refrigerant, two different groups of tests are carried out in the working conditions shown in Table 4. The first group of tests (Run 1-5 in Table 4) is oriented at analysing the heat pump performance keeping constant the compressor shaft rotational frequency and under the same temperature conditions at the inlet and the outlet of the evaporator and of the condenser. Due to different system performance with different refrigerants and different operating conditions, during these test the secondary fluid mass flow rates are adjusted in order to match the desired temperature at heat exchangers inlet and outlet.
The second group of tests (Run 6-10 in Table 4) is aimed at identifying the compressor shaft rotational frequency that leads to the same heating capacity delivered by the heat pump in the baseline configuration, i.e. with the R134a as working fluid and considering a shaft frequency equal to 50 Hz. Indeed, as shown further in the text, the results of the first group of tests show that heat pump heating capacity reduces when the two HFOs are used. Therefore, the performance of the system under the constraint of equal condenser heat transfer rate are investigated.

Table 4. Experimental conditions.

Run	f	Evaporator			Condenser		
		$\dot{m}_G$ [kg·h^{-1}]	$T_{G,IN}$	$T_{G,OUT}$	$\dot{m}_W$ [kg·h^{-1}]	$T_{W,IN}$	$T_{W,OUT}$
1	50 Hz	Identified	10 °C	5 °C	Identified	30 °C	35 °C
2	50 Hz	Identified	10 °C	5 °C	Identified	40 °C	45 °C
3	50 Hz	Identified	10 °C	5 °C	Identified	50 °C	55 °C
4	50 Hz	Identified	10 °C	5 °C	Identified	60 °C	65 °C
5	50 Hz	Identified	10 °C	5 °C	Identified	70 °C	75 °C
6	Variable	Same as R134a	10 °C	5 °C	Same as R134a	30 °C	35 °C
7	Variable	Same as R134a	10 °C	5 °C	Same as R134a	40 °C	45 °C
8	Variable	Same as R134a	10 °C	5 °C	Same as R134a	50 °C	55 °C

9	Variable	Same as R134a	10 °C	5 °C	Same as R134a	60 °C	65 °C
10	Variable	Same as R134a	10 °C	5 °C	Same as R134a	70 °C	75 °C

The condenser heating capacity as a function of water temperature at condenser outlet for the three refrigerants tested and for a compressor shaft frequency equal to 50 Hz is depicted in Figure 2. The results show that, in a pure drop-in application, the use of low GWP alternatives to R134a leads to an overall reduction of the condenser heat transfer rate. Indeed, with R1234yf a slight condenser capacity reduction in the range 3.80% - 9.80% is found whereas the use of R1234ze(E) leads to a substantial capacity reduction, in the range 20.96% - 23.07%. This behaviour arises mainly from the different thermophysical properties of the two HFO refrigerants, being the enthalpy difference across the condenser lower than that of the R134a, due to higher molar mass, and, for the R1234ze(E) only, the refrigerant mass flow rate strongly different, due to a lower density at compressor suction.

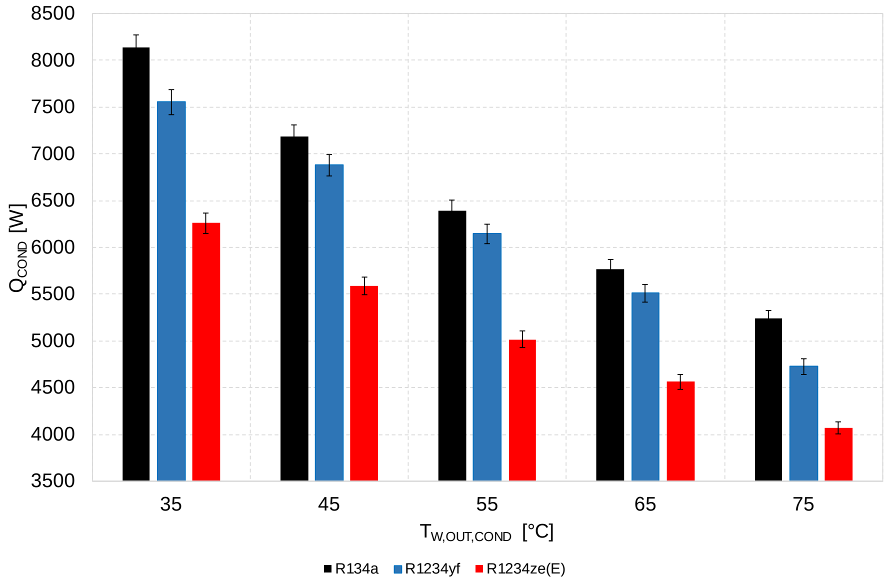

Figure 2. Condenser capacity as a function of water temperature at condenser outlet for R134a, R1234yf and R1234ze(E).

The heat pump COPs for the same testing conditions are shown in Figure 3. The use of R1234yf leads to a reduction of COP in the range 1.46% - 6.14%, whereas a very slight reduction in the range 0.59% - 2.50% is found with R1234ze(E). This behaviour is related to the different critical temperatures and molar masses of the two HFO with respect to R134a. Indeed, as shown in [13], the COP of a vapour compression system increases if high critical temperature and low molar mass refrigerant is used. As shown in Table 3, the critical temperature and the molar mass of R1234yf are respectively lower than and higher than those of R134a which, in turn, leads to lower COP. Conversely, both the critical temperature and the molar mass of R1234ze(E) are higher than those of R134a. From the COP point of view, these two properties act in opposite directions, eventually resulting in a low reduction of the performance index with respect to the R134a configuration.

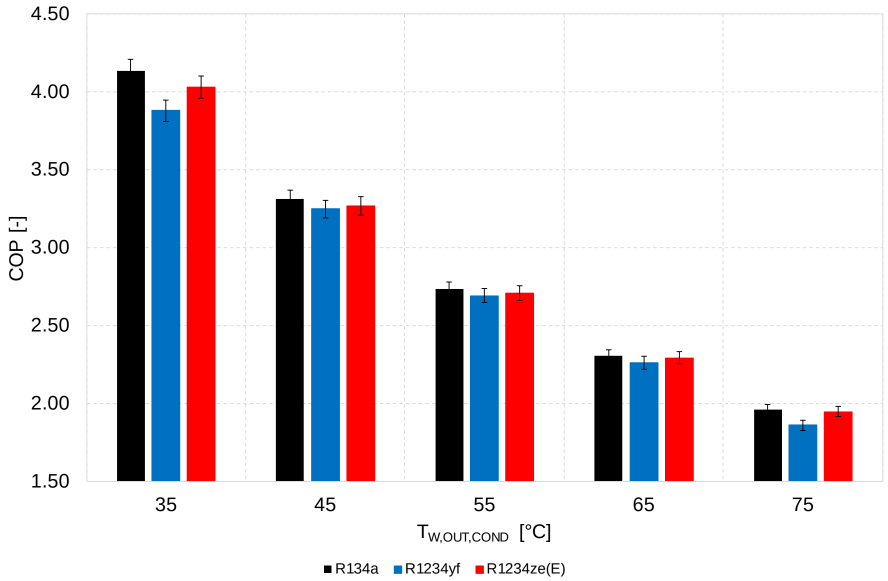

Figure 3. Heat pump COP as a function of water temperature at condenser outlet for R134a, R1234yf and R1234ze(E).

The rotational frequencies of the compressor shaft needed to deliver the same condenser heating capacity given with R134a as a function of water temperature at condenser outlet are shown in Figure 4. In this figure, the frequency of the heat pump working with R134a is reported too for reference. An increase of the shaft frequency in the range 5.21% - 16.52% is found when the heat pump is charged with R1234yf, whereas with the use of R1234ze(E) an increase in the range 32.39% - 50.26% is needed. These results agree with those reported in Figure 2 where smaller differences between the heating capacities of R134a and R1234yf and larger values with R1234ze(E) are shown. Therefore, it is expected that the smaller the condenser heat transfer rate difference, the lower the shaft frequency increase and vice-versa. It is worth noting that the point at $T_{W,OUT,COND}$ = 75 °C with R1234yf is out of the envelope of the compressor since the condensing temperature is slightly higher than 80 °C.

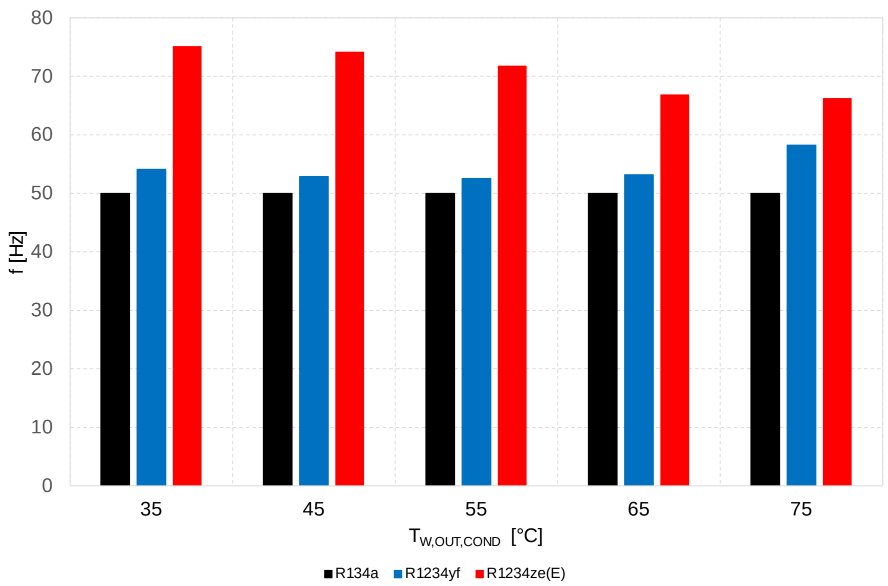

Figure 4. Compressor shaft frequency needed to deliver the baseline capacity as a function of water temperature at condenser outlet for R134a (baseline), R1234yf and R1234ze(E).

Finally, the COPs of the heat pump at the modified rotational frequency of the compressor shaft are shown in Figure 5. As expected, an increase in rotational frequency causes an increase in mass flow rate which, in turn, forces the evaporating and condensing temperatures to separate and the COP to reduce. The COP reduction is in the range 2.77% - 7.38% with R1234yf and 1.25% - 18.11% with R1234ze(E). At low water temperatures at condenser outlet, the COP reduction of the R1234ze(E) system is so high that it performs worse than the R1234yf system, but the trend reverses increasing the water temperature at condenser outlet since the R1234yf is approaching the critical temperature.

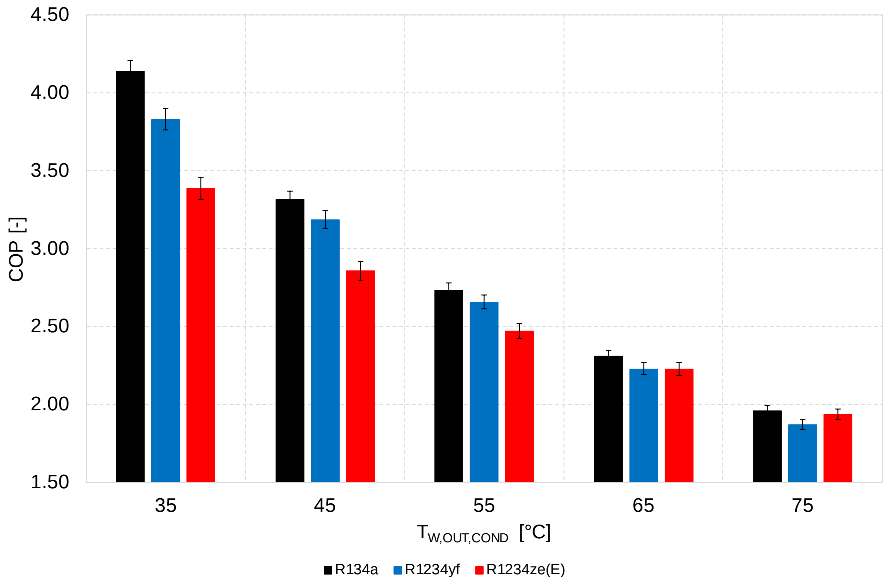

Figure 5. Heat pump COP as a function of water temperature at condenser outlet for R134a, R1234yf and R1234ze(E) when the heat pump capacity is equal to the one of the baseline.

4. Conclusions

In the present paper, the first experimental results of the use of R134a and its low GWP alternatives R1234yf and R1234ze(E) in a water-to-water heat pump in a drop-in application are presented. The heat pump is first tested with R134a to establish a baseline performance and, then, is tested under the same water temperatures at evaporator and condenser inlets and outlets. The results show that the use of R1234yf leads to a slight capacity reduction, in the range 3.80% - 9.80%, and a COP reduction, in the range 1.46% - 6.14% while a substantial capacity reduction, in the range 20.96% - 23.07%, and a negligible COP reduction, in the range 0.59% - 2.50%, are found with R1234ze(E).

The analysis of the compressor shaft rotational frequency needed to match the same heating capacity of R134a is also carried out. Increases up to 17% and 50% are respectively found for R1234yf and R1234ze(E), but subsequent reductions of heat pump COP up to 7.38% and 18.11% arise.

Nomenclature

COP Coefficient of performance [-]
c_P Isobaric heating capacity [J·kg^{-1}·K^{-1}]
h Enthalpy [J·kg^{-1}]
$\dot{m}$ Mass flow rate [kg·s^{-1}]
$\dot{Q}$ Heat flow rate [W]
T Temperature [°C]
t_{95} Student test multiplier at 95% confidence [-]
u Uncertainty [-]
$\dot{W}$ Power [W]

Greek symbols
$\sigma_{\bar{x}}$ Standard deviation of the mean value [-]

Subscripts
$COMP$ Compressor
$COND$ Condenser
IN Inlet
$INST$ Instrumental
OUT Outlet
R Refrigerant
W Water

Acknowledgments
The financial support of MIUR through the program PRIN 2015 (Grant Number 2015M8S2PA) is greatly acknowledged. The company Frascold S.p.A. is acknowledged for providing the compressor used in the experimental campaign. The company Rivoira Refrigerants S.r.l. is acknowledged for providing the sample of R1234yf.

References

[1] European Union 2014 Regulation (EU) No 517/2014 of the European Parliament and the Council of 16 April 2014 on fluorinated greenhouse gases and repealing Regulation (EC) No 842/2006 Off. J. Eur. Union 150 195-230
[2] United Nations Environment Programme 2016
[3] Jarall S 2012 *Int. J. Refrig.* **35** 1668-77
[4] Navarro-Esbrí J, Mendoza-Miranda J M, Mota-Babiloni A, Barragán-Cervera A and Belman-Flores J M 2013 *Int. J. Refrig.* **36** 870-80
[5] Mota-Babiloni A, Navarro-Esbrí J, Barragán Á, Molés F and Peris B 2014 *Appl. Therm. Eng.* **71** 259-65
[6] Janković Z, Sieres Atienza J and Martínez Suárez J A 2015 *Appl. Therm. Eng.* **80** 42-54
[7] Sánchez D, Cabello R, Llopis R, Arauzo I, Catálan-Gil J and Torrella E 2017 *Int. J. Refrig.* **74** 269-82
[8] Nawaz K, Shen B, Elatar A, Baxter V and Abdelaziz O 2017 *Int. J. Refrig.* **82** 348-65
[9] Devecioğlu A T and Oruç V 2018 *Energy* **155** 105-16
[10] Lemmon E W, Huber M L and McLinden M O 2013 NIST Standard Reference Database 23: Reference Fluid Thermodynamic and Transport Properties-REFPROP, Version 9.1 *National Institute of Standards and Technology, Standard Reference Data Program* (Gaithersburg, MD, USA)
[11] Moffat R J 1988 *Exp. Therm. Fluid Sci.* **1** 3-17
[12] IPCC 2013 *Climate Change 2013: The Physical Science Basis. Contribution of Working Group I to the Fifth Assessment Report of the Intergovernmental Panel on Climate Change* ed T F Stocker, D Qin, G-K Plattner, M Tignor, S K Allen, J Boschung, A Nauels, Y Xia, V Bex and P M Midgley (Cambridge United Kingdom and New York NY USA: Cambridge University Press) p 732
[13] Domanski P A, Brown J S, Heo J, Wojtusiak J and McLinden M O, 2014 *Int. J. Refrig.* **38** 71-9